Semantic Priming and Repetition Suppression

Introduction

Repetition suppression has been previously used to study the specificity of orthographic representations of words in the visual word form area (VWFA). “fMRI repetition suppression (also termed fMRI adaptation) relies on the fact that neurons show suppression in their response to repeated presentation of stimuli or information to which they are sensitive” (Barron, Garvert, and Behrens, 2016). In Glezer, Jiang, and Riesenhuber (2009), the authors did not observe a repetition suppression effect when successively-presented prime words and target words that differed by one letter were real words as opposed to pseudowords, supporting the hypothesis that individual words are represented as distinct wholes even if they have a high degree of orthographic overlap. The authors also concluded a supplementary study where they tested if the repetition suppression effect was due to semantic effects (supplementary study); they found a robust semantic priming effect behaviorally, but no repetition suppression in the VWFA.

Beyond the VWFA, experience-dependent maps have been found in the human brain for various visual features (Wandell & Winawer, 2011), cognitive states (Yarkoni et al., 2011), and semantic representations. However, repetition suppression has not been used to investigate semantic representations. Semantic cortical maps have been previously generated by getting participants to listen to stories (Huth et al., 2016; Zhang et al., 2020), as well as watching silent movies (Popham et al., 2021).

Methods

3 participants completed 232 trials across four conditions, with each trial constructed in the same way as the original study. Each trial will include the presentation of two successive words, and each of the two words will be presented for 300ms and separated by a 400ms blank screen, followed by a 3080ms blank screen, bringing the total trial time to 4.08 seconds. A behavioural response within the 3080ms window terminated the trial immediately and initiated the start of the next trial.

Due to varying amounts of scanner time available across different sessions and technical difficulties extracting behavioural responses through the fibre optic response pads (FORP), 2 of the participants completed the full 232 trials and 1 participant completed 85 trials. Of the 2 participants who completed the full trials, behavioural responses were available for 1 participant.

The four experimental conditions were:

1. Same prime and target words (e.g. boat – boat)
2. Prime and target words are orthographically dissimilar but semantically similar (e.g. boat – ship)
3. Prime and target words differ by one letter but are semantically unrelated (e.g. boat – goat)
4. Prime and target words are different orthographically and semantically (e.g. goat – ship).

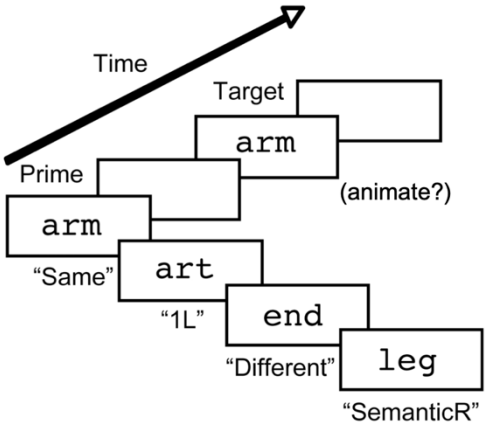

Participants had to make a judgment on animacy (animate/inanimate) on every trial upon presentation of the target word and make a behavioral response.

Neuroimaging was performed at the Stanford University Center for Cognitive and Neurobiological Imaging using a GE Ultra High Performance 3T scanner. Scan parameters were designed to accelerate image acquisition and improve signal to noise ratio via a single-echo echo planar imaging (EPI) sequence. Repetition time was set at 1250ms, with right to left phase-encoding direction, yielding brain volumes with voxel size of 1mm x 0.9mm x 0.9mm. Details of anatomical and functional neuroimaging data preprocessing in the form of fMRIPrep boilerplate text are included as appendices.

Subject-level BOLD responses were standardized and detrended, and the first-level Nilearn model was fitted using the subject's individual brain mask, the Glover hemodynamic response function, a third order polynomial drift model, the events file for each subject, as well as subject-level confounds (six head motion parameters in the three directions, and the global_signal, csf, and white_matter variables).

Whole-brain first-level standardized contrasts were constructed with a Z-score signal threshold of 2, which would correspond to approximately to a significance level (p-value) of 0.05 for a two-tailed test.

Due to the variation in experimental protocol for 3 participants and the small sample size, we did not expect to find any meaningful group level comparisons. Confirmatory analysis using a whole-brain second-level Nilearn model fitted with the same contrast matrices did not yield any results, and are thus not further reported.

Based on Caffarra and Karipidis et al. (2021), the VWFA mask was defined as a sphere centered at (-45, -55, -12) in MNI coordinates with a radius of 8 voxels to include the coordinates bounded by the black box below.

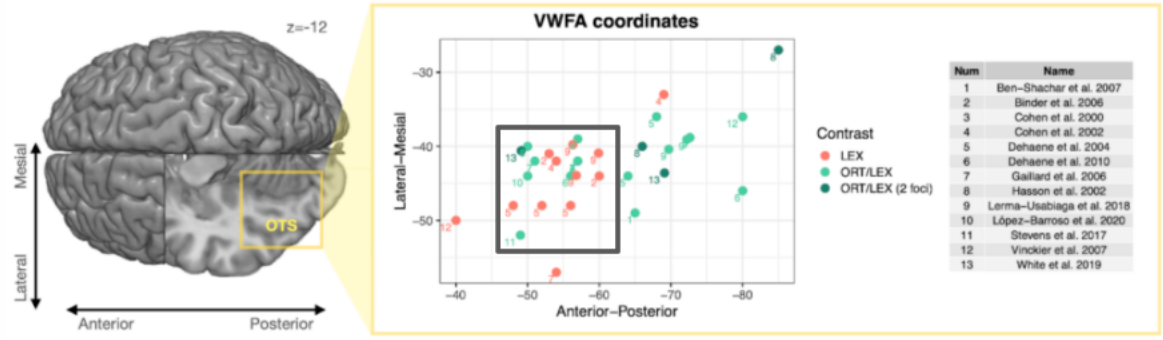

To compute the amount of signal change relative to the fixation baseline, the whole-brain BOLD signal was masked using the VWFA mask defined above, and the mean activation within the region of interest (ROI) was averaged at each time point.

Due to the HRF, the BOLD signal in the ROI at any time point would be influenced not just by the immediate trial, but by previous trials to various extents, as can be seen in the overlapping events in the design matrix on the right. Thus, the mean BOLD signal within the ROI at each time point was tagged to the condition with the highest contribution.

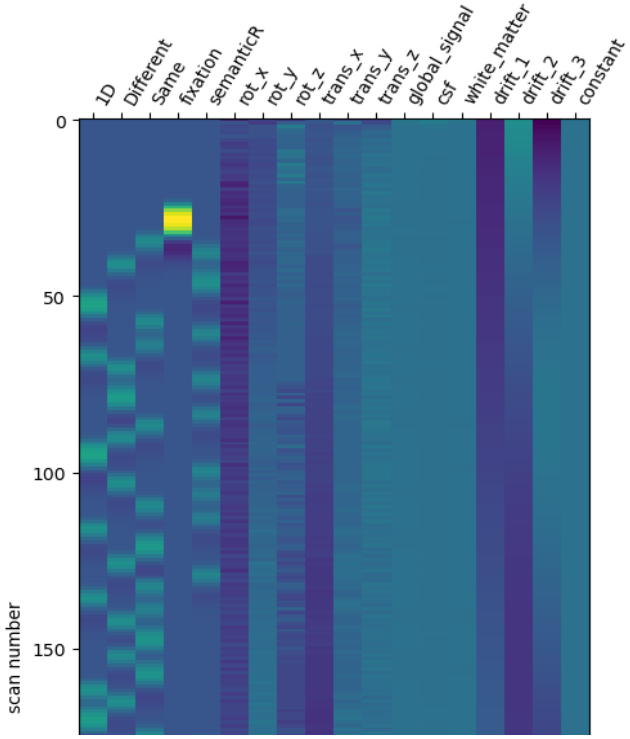

This yielded a matrix with two columns, one with the value of the mean BOLD signal in the ROI, as well as a second column that indicated which condition this BOLD signal had been tagged to. The BOLD signals for each condition were then aggregated to compute the mean and standard error.

Code for the analysis and all data files (excluding the neuroimaging files) are available at https://github.com/chiuhoward/EDUC464.

Results

The table below provides a summary of the 3 participants and the variables relevant to the interpretation of the results.

Participant ID	Trial Duration	Number of Trials Completed
4641	4.08s	232
4643	4.08s	85
4644	Variable (due to behavioural responses)	232

We completed the following analyses:

1. analyzed behavioural data for participant 4644 (accuracy and reaction times)
2. subject-level whole-brain contrasts in three conditions (all visual stimuli versus baseline, identical stimuli versus other visual stimuli, and semantically-related stimuli versus orthographically-related stimuli)
3. subject-level BOLD responses in the visual word form area across the four conditions relative to the fixation baseline.

The participant had accuracy close to ceiling, with a pooled accuracy of 97.8% (227/232 trials) on the animacy judgments of target words. We observed the presence of a priming effect, with a significant difference in reaction times across conditions ($F = 4.15$, $p = 0.007$).

A post-hoc Tukey's honestly significant difference (HSD) test showed that there was a statistically significant difference between the Same – 1D ($p = 0.04$) and semanticR – same ($p = 0.008$) conditions. The other comparisons were not statistically significant.

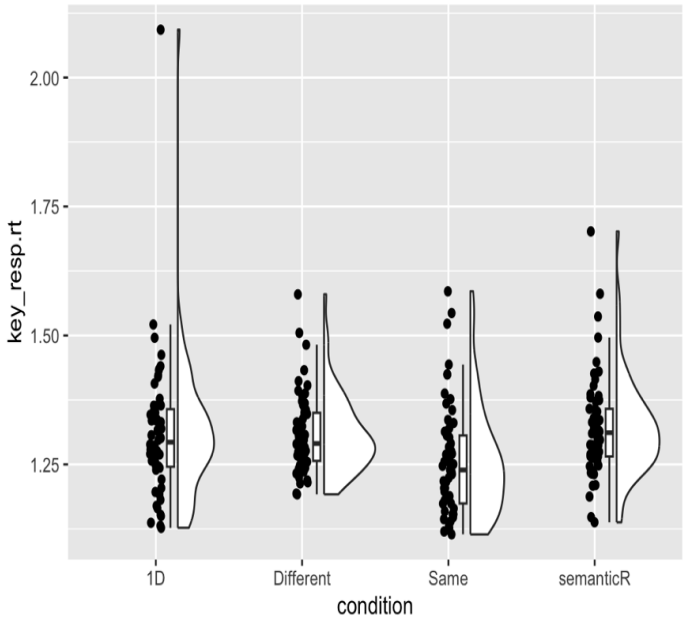

The first contrast we looked at was all visual conditions compared to the fixation baseline. We observed some positive contrast near the ROI, as well as some activation across the early visual cortices. This contrast was stronger for the subjects who had completed more trials, but there was still noise distributed throughout.

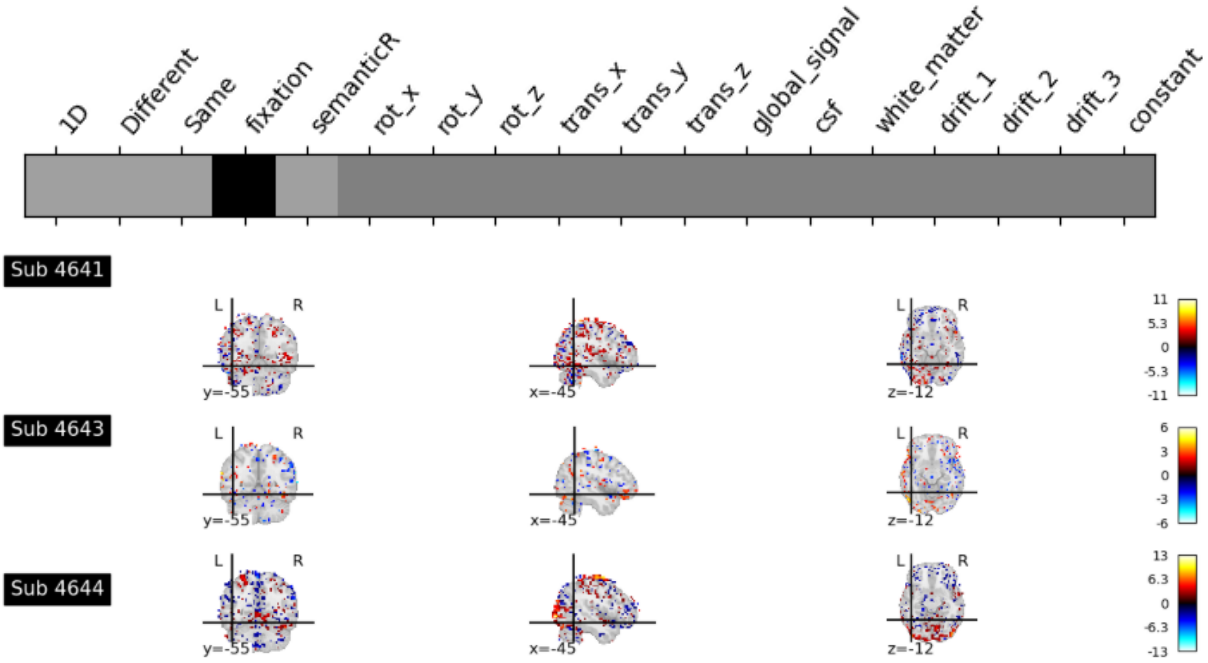

In the second contrast, the hypothesized contrast for identical stimulus versus all other visual conditions would be that the other conditions would have a lower degree of repetition suppression and thus have a higher BOLD signal. Although there was no significant contrast in the voxel at the center of the VWFA mask, there are voxels in the surrounding region that could potentially be within the ROI. However, these contrasts are in the opposite direction of what was hypothesized.

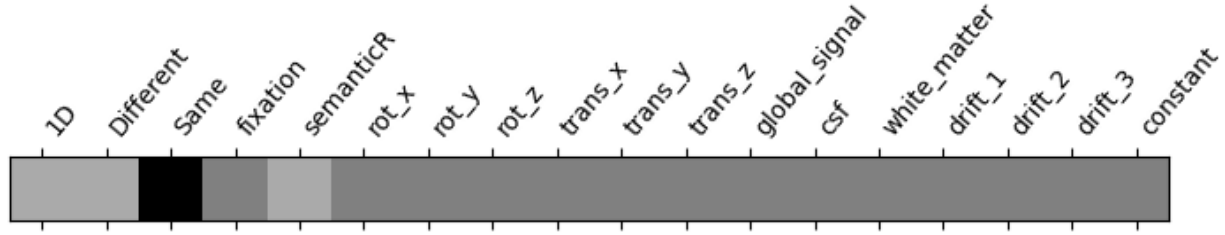

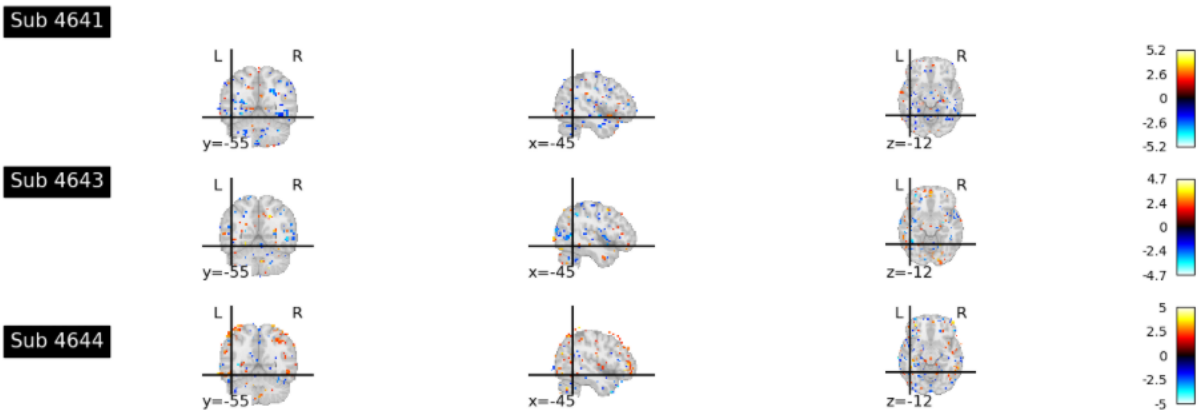

In the last contrast, we are looking for areas that show semantically-related repetition suppression effects. There was contrast in the expected positive direction in left parietal and occipital regions, but also noise distributed throughout.

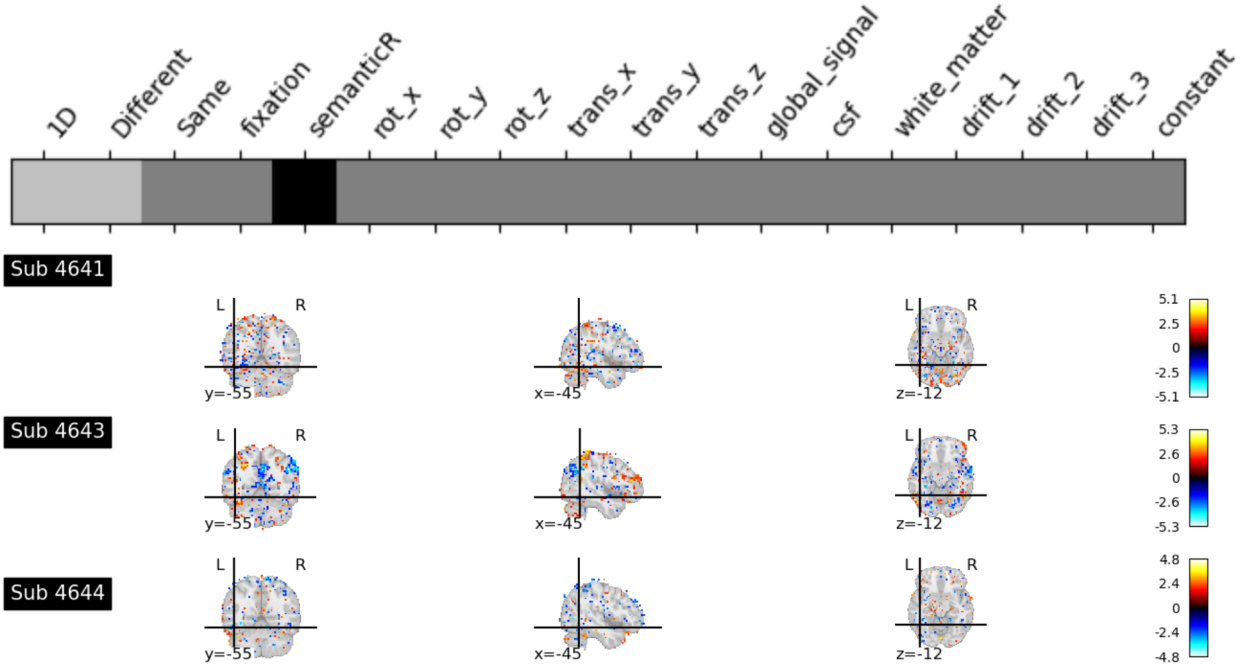

For the extent of BOLD signal change in the different conditions relative to baseline, there was no consistent pattern. Only one participant (sub-4643) had contrasts in the expected direction (all higher than the fixation baseline), and there was no repetition suppression observed in that participant as compared to the result of the original experiment (top left corner of figure below).

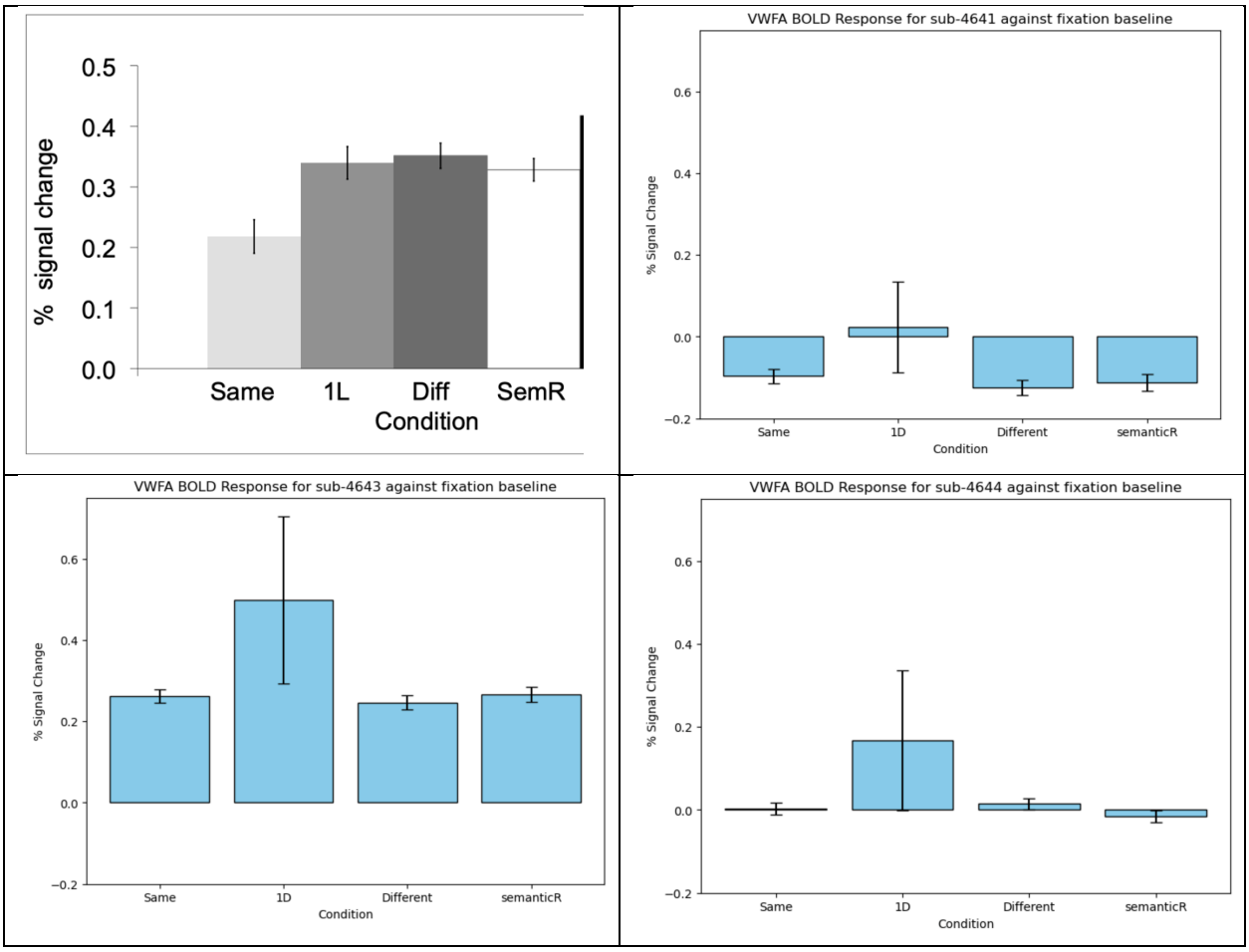

Discussion

Although we did observe a robust priming effect in the identical condition, the order of reaction times in the other conditions was different from the hypothesized order of Same < SemanticR < 1D < Different. The priming effect could possibly due to a combination of orthography and semantics, with top-down and task-dependent contributions of each dimension.

The results of the neuroimaging analyses were noisy, and no robust conclusions can be drawn from the observations. It was difficult to replicate even well-established findings in the literature (e.g. widespread activation of visual cortex in response to visual stimuli).

Beyond the obvious limitation of saple size, I would have to give more thought to the contrasts used in my task paradigm, and also protocol design for neuroimaging. I learnt that localizers are often run as a separate experiment to the experimental task. I would also need more blank screen/fixation time to get a more robust baseline that I can compare activation in the other conditions with.

References

Barron, H. C., Garvert, M. M., & Behrens, T. E. J. (2016). Repetition suppression: A means to index neural representations using BOLD? *Philosophical Transactions of the Royal Society B: Biological Sciences*, *371*(1705), 20150355. https://doi.org/10.1098/rstb.2015.0355

Glezer, L. S., Jiang, X., & Riesenhuber, M. (2009). Evidence for Highly Selective Neuronal Tuning to Whole Words in the "Visual Word Form Area." *Neuron*, *62*(2), 199–204. https://doi.org/10.1016/j.neuron.2009.03.017

Caffarra, S., Karipidis, I. I., Yablonski, M., & Yeatman, J. D. (2021). Anatomy and physiology of word-selective visual cortex: From visual features to lexical processing. *Brain Structure and Function*, *226*(9), 3051–3065. https://doi.org/10.1007/s00429-021-02384-8

Esteban, O., Markiewicz, C. J., Blair, R. W., Moodie, C. A., Isik, A. I., Erramuzpe, A., Kent, J. D., Goncalves, M., DuPre, E., Snyder, M., Oya, H., Ghosh, S. S., Wright, J., Durnez, J., Poldrack, R. A., & Gorgolewski, K. J. (2019). fMRIPrep: A robust preprocessing pipeline for functional MRI. *Nature Methods*, *16*(1), 111–116. https://doi.org/10.1038/s41592-018-0235-4

Gorgolewski, K., Burns, C. D., Madison, C., Clark, D., Halchenko, Y. O., Waskom, M. L., & Ghosh, S. S. (2011). Nipype: A Flexible, Lightweight and Extensible Neuroimaging Data Processing Framework in Python. *Frontiers in Neuroinformatics*, *5*. https://doi.org/10.3389/fninf.2011.00013

Huth, A. G., De Heer, W. A., Griffiths, T. L., Theunissen, F. E., & Gallant, J. L. (2016). Natural speech reveals the semantic maps that tile human cerebral cortex. *Nature*, *532*(7600), 453–458. https://doi.org/10.1038/nature17637

Popham, S. F., Huth, A. G., Bilenko, N. Y., Deniz, F., Gao, J. S., Nunez-Elizalde, A. O., & Gallant, J. L. (2021). Visual and linguistic semantic representations are aligned at the border of human visual cortex. *Nature Neuroscience*, *24*(11), 1628–1636. https://doi.org/10.1038/s41593-021-00921-6

Wandell, B. A., & Winawer, J. (2011). Imaging retinotopic maps in the human brain. *Vision Research*, *51*(7), 718–737. https://doi.org/10.1016/j.visres.2010.08.004

Yarkoni, T., Poldrack, R. A., Nichols, T. E., Van Essen, D. C., & Wager, T. D. (2011). Large-scale automated synthesis of human functional neuroimaging data. *Nature Methods*, *8*(8), 665–670. https://doi.org/10.1038/nmeth.1635

Zhang, Y., Han, K., Worth, R., & Liu, Z. (2020). Connecting concepts in the brain by mapping cortical representations of semantic relations. *Nature Communications*, *11*(1), 1877. https://doi.org/10.1038/s41467-020-15804-w

Appendix – fMRIPrep boilerplate text

Results included in this manuscript come from preprocessing performed using *fMRIPrep* 23.1.3 (Esteban et al. (2019); Esteban et al. (2018); RRID:SCR_016216), which is based on *Nipype* 1.8.6 (K. Gorgolewski et al. (2011); K. J. Gorgolewski et al. (2018); RRID:SCR_002502).

Anatomical data preprocessing

A total of 1 T1-weighted (T1w) images were found within the input BIDS dataset. The T1-weighted (T1w) image was corrected for intensity non-uniformity (INU) with N4BiasFieldCorrection (Tustison et al. 2010), distributed with ANTs (version unknown) (Avants et al. 2008, RRID:SCR_004757), and used as T1w-reference throughout the workflow. The T1w-reference was then skull-stripped with a *Nipype* implementation of the antsBrainExtraction.sh workflow (from ANTs), using OASIS30ANTs as target template. Brain tissue segmentation of cerebrospinal fluid (CSF), white-matter (WM) and gray-matter (GM) was performed on the brain-extracted T1w using fast (FSL (version unknown), RRID:SCR_002823, Zhang, Brady, and Smith 2001). Brain surfaces were reconstructed using recon-all (FreeSurfer 7.3.2, RRID:SCR_001847, Dale, Fischl, and Sereno 1999), and the brain mask estimated previously was refined with a custom variation of the method to reconcile ANTs-derived and FreeSurfer-derived segmentations of the cortical gray-matter of Mindboggle (RRID:SCR_002438, Klein et al. 2017). Volume-based spatial normalization to one standard space (MNI152NLin2009cAsym) was performed through nonlinear registration with antsRegistration (ANTs (version unknown)), using brain-extracted versions of both T1w reference and the T1w template. The following template was selected for spatial normalization and accessed with *TemplateFlow* (23.0.0, Ciric et al. 2022): *ICBM 152 Nonlinear Asymmetrical template version 2009c* [Fonov et al. (2009), RRID:SCR_008796; TemplateFlow ID: MNI152NLin2009cAsym].

Functional data preprocessing

For each of the BOLD runs found per subject (across all sessions), the following preprocessing was performed. First, a reference volume and its skull-stripped version were generated using a custom methodology of *fMRIPrep*. Head-motion parameters with respect to the BOLD reference (transformation matrices, and six corresponding rotation and translation parameters) are estimated before any spatiotemporal filtering using mcflirt (FSL , Jenkinson et al. 2002). BOLD runs were slice-time corrected to 0.598s (0.5 of slice acquisition range 0s-1.2s) using 3dTshift from AFNI (Cox and Hyde 1997, RRID:SCR_005927). The BOLD time-series (including slice-timing correction when applied) were resampled onto their original, native space by applying the transforms to correct for head-motion. These resampled BOLD time-series will be referred to as *preprocessed BOLD in original space*, or just *preprocessed BOLD*. The BOLD reference was then co-registered to the T1w reference using bbregister (FreeSurfer) which

implements boundary-based registration (Greve and Fischl 2009). Co-registration was configured with six degrees of freedom. Several confounding time-series were calculated based on the *preprocessed BOLD*: framewise displacement (FD), DVARS and three region-wise global signals. FD was computed using two formulations following Power (absolute sum of relative motions, Power et al. (2014)) and Jenkinson (relative root mean square displacement between affines, Jenkinson et al. (2002)). FD and DVARS are calculated for each functional run, both using their implementations in *Nipype* (following the definitions by Power et al. 2014). The three global signals are extracted within the CSF, the WM, and the whole-brain masks. Additionally, a set of physiological regressors were extracted to allow for component-based noise correction (*CompCor*, Behzadi et al. 2007). Principal components are estimated after high-pass filtering the *preprocessed BOLD* time-series (using a discrete cosine filter with 128s cut-off) for the two *CompCor*variants: temporal (tCompCor) and anatomical (aCompCor). tCompCor components are then calculated from the top 2% variable voxels within the brain mask. For aCompCor, three probabilistic masks (CSF, WM and combined CSF+WM) are generated in anatomical space. The implementation differs from that of Behzadi et al. in that instead of eroding the masks by 2 pixels on BOLD space, a mask of pixels that likely contain a volume fraction of GM is subtracted from the aCompCor masks. This mask is obtained by dilating a GM mask extracted from the FreeSurfer's *aseg* segmentation, and it ensures components are not extracted from voxels containing a minimal fraction of GM. Finally, these masks are resampled into BOLD space and binarized by thresholding at 0.99 (as in the original implementation). Components are also calculated separately within the WM and CSF masks. For each CompCor decomposition, the *k* components with the largest singular values are retained, such that the retained components' time series are sufficient to explain 50 percent of variance across the nuisance mask (CSF, WM, combined, or temporal). The remaining components are dropped from consideration. The head-motion estimates calculated in the correction step were also placed within the corresponding confounds file. The confound time series derived from head motion estimates and global signals were expanded with the inclusion of temporal derivatives and quadratic terms for each (Satterthwaite et al. 2013). Frames that exceeded a threshold of 0.5 mm FD or 1.5 standardized DVARS were annotated as motion outliers. Additional nuisance timeseries are calculated by means of principal components analysis of the signal found within a thin band (*crown*) of voxels around the edge of the brain, as proposed by (Patriat, Reynolds, and Birn 2017). The BOLD time-series were resampled into standard space, generating a *preprocessed BOLD run in MNI152NLin2009cAsym space*. First, a reference volume and its skull-stripped version were generated using a custom methodology of *fMRIPrep*. All resamplings can be performed with *a single interpolation step* by composing all the pertinent transformations (i.e. head-motion transform matrices, susceptibility distortion correction when available, and co-registrations to anatomical and output spaces). Gridded (volumetric) resamplings were performed usingantsApplyTransforms (ANTs), configured with Lanczos interpolation to minimize the smoothing effects of other kernels (Lanczos 1964). Non-gridded (surface) resamplings were performed using mri_vol2surf (FreeSurfer).

Many internal operations of *fMRIPrep* use *Nilearn* 0.10.1 (Abraham et al. 2014, RRID:SCR_001362), mostly within the functional processing workflow. For more details of the pipeline, see the section corresponding to workflows in *fMRIPrep*'s documentation.